# Marginal Stability and Chaos in Coupled Faults Modeled by Nonlinear Circuits

Stuart Field, Naia Venturi, and Franco Nori
*Department of Physics, The University of Michigan, Ann Arbor, Michigan 48109-1120*
(Received 7 July 1994)

Studies of slider-block systems, used for decades to model the interactions between geological fault segments, have been mostly theoretical due to the difficulty in producing well-controlled mechanical systems which mimic these models' dynamics. We present here an experimental study of the dynamics of two elastically coupled slider blocks, using an electronic circuit with highly nonlinear load-unload elements. Unlike earlier computer simulations, a nominally symmetric circuit exhibits several alternating periodic and chaotic solutions as a function of the coupling parameter, emphasizing the importance of experimental studies in understanding this model.

PACS numbers: 05.45.+b, 05.40.+j, 91.30.Px

During the past three decades, there have been many studies of spring-loaded slider-block models of fault dynamics (see, for example, Refs. [1–5], and references therein). These models consist of slider blocks coupled by elastic springs to each other and to a constant-velocity driver; as the blocks slide, they are subject to both static and velocity-weakening dynamical friction forces. Crucial elements of earthquake dynamics, including elastic storage of energy and friction-controlled loading-unloading behavior, are incorporated in these nonstochastic mechanical models. Dynamical instabilities originating from nonlinear friction forces have been studied using both single- and two-block models; the latter are low-dimensional analogs to tectonic deformation. Symmetric two-block mass-spring models can produce spatially asymmetric dynamics [6]. Asymmetric models, e.g., with different friction forces on each block, exhibit chaos for certain parameter ranges [7,8].

Dynamical systems with few block sliders are important for several reasons. First, they deliberately emphasize the effect of boundaries, which are essential to model features of natural seismicity [9]. In fact, recent investigations [7] indicate that the dynamics of two coupled slider blocks is much like that observed in geological slip faults. Second, the presence of chaotic behavior in a low-dimensional system often implies chaotic dynamics in similar higher-dimensional systems.

The vast majority of these investigations on slider blocks have been theoretical, because it is not easy to produce a well-controlled and easy-to-monitor laboratory system with mechanical components. Electronic circuits, however, provide a convenient and useful system to study complex dynamical behavior [10,11]. Their increasingly widespread use and appeal are due in part to their economy, accessibility of parts, simplicity, ease of implementation, and versatility. Electronic circuits are easy to modify, with many nonlinear friction laws available with simple variations in components. These circuits are also characterized by high bandwidths, allowing the long data runs needed to obtain statistically meaningful results. As much as $10^6$ events, instead of a few hundred, can be monitored in real time as parameters are changed. Finally, circuits are a very well-characterized system, in contrast to mechanical structures, and can be used to experimentally test whether theoretical predictions are robust to changes in component values and to noise, both unavoidably present in real physical systems. Circuits, while close to ideal, are nonetheless real-world experiments, and so results obtained will have proven robustness.

With these ideas in mind, we have constructed a circuit specifically designed to be the electronic analog of a two-block mechanical system. Electrical quantities corresponding to mechanical variables such as position and velocity may be conveniently measured in this circuit. We find that the circuit dynamics is not smooth, but exhibits bursts, even though the circuit is driven by a low dc voltage. Furthermore, as its parameters are varied, the circuit displays a wide range of interesting dynamical behavior, including alternating regions of periodicity and chaos. This dynamics is reminiscent of the ones found in chemical reactions and glow discharges [12].

The circuit investigated is of a simple *L-C* design with the important addition of a *highly* nonlinear resistive element (see Fig. 1). For ideal components, its dynamics is governed by the equations

$$C\ddot{X}_1 + \left\{\frac{1}{L} + \frac{1}{L_c}\right\}X_1 - \frac{1}{L_c}X_2 = -I_1(\dot{X}_1 + V_d), \quad \text{(1a)}$$

$$C\ddot{X}_2 + \left\{\frac{1}{L} + \frac{1}{L_c}\right\}X_2 - \frac{1}{L_c}X_1 = -I_2(\dot{X}_2 + V_d), \quad \text{(1b)}$$

where $C$ denotes the capacitance, $L$ and $L_c$ inductances, and $I(\dot{X})$ the nonlinear current-voltage or *I-V* relation shown in Fig. 1. $X$ is defined by $X_i \equiv \int(V_i - V_d)dt$, so that $\dot{X}_i = V_i - V_d$. Here, $V_i$ is the voltage at node $i$ and $V_d$ is the driving voltage in Fig. 1.

A direct analogy may be drawn between the dynamics of this circuit and the two-block mechanical model used in studies of earthquake dynamics. The equations of motion for the latter system are given by [7]

 0031-9007/95/74(1)/74(4)$06.00 

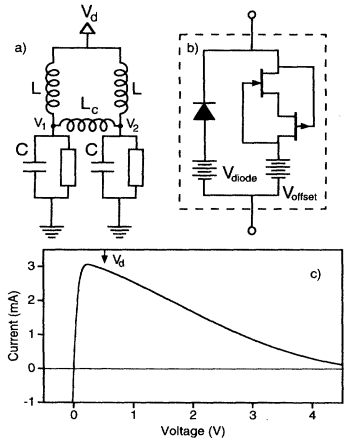


FIG. 1. (a) Schematic diagram of the circuit used. The nonlinear element, shown as an open box, is described in (b), and has the $I$-$V$ characteristics shown in (c). The circuit parameters used here are $V_d = 0.52$ V, $C = 2.2$ nF, $L = 5$ mH, 2.3 mH $\leq L_c \leq$ 6.5 mH, $V_{\text{diode}} = 0.64$ V, and $V_{\text{offset}} = -4.2$ V. The arrow in (c) indicates the value of $V_d$ used.

$$m\ddot{y}_1 + (k + k_c)y_1 - k_c y_2 = -F_1(\dot{y}_1 + v_d), \quad (2a)$$

$$m\ddot{y}_2 + (k + k_c)y_2 - k_c y_1 = -F_2(\dot{y}_2 + v_d), \quad (2b)$$

where $F_1$ and $F_2$ are the friction forces acting on two masses $m$, coupled to a driver moving at a very small velocity $v_d$ by springs of strength $k$, extended by distances $y_1$ and $y_2$ (see Fig. 1 in Ref. [7]). The blocks are elastically coupled to each other by a spring of strength $k_c$. The velocity-weakening force, $F = F(\dot{y})$, is a decreasing function of the velocity $\dot{y}$.

Note that the two systems of equations above are identical in form. Consequently, we say that the circuit in Fig. 1 is an electrical analog of the two slider-block system shown in Fig. 1 of Ref. [7], provided we identify the analogous entries listed in the columns of Table I. This dictionary is useful because the behavior of the circuit can be given a clear physical interpretation if we think in terms of its mechanical analog. Thus in this paper we will often refer to a capacitor as "a block," an inductor as "a spring," the voltage at node 1 as "block 1's velocity," and so on. This ability to think about the electronic circuit's behavior in terms of its mechanical analog is a particularly appealing aspect of this circuit.

Three important parameters determine the behavior of the electronic and mechanical systems described above: the ratio $\beta$ of the frictional forces of the two blocks, or equivalently, the ratio of the $I$-$V$ curves: $\beta = F_2(\dot{y})/F_1(\dot{y}) = I_2(V)/I_1(V)$; the strength of the coupling, $\alpha = k_c/k = L/L_c$; and the rate of decay $\gamma$ of the friction force, or of the $I$-$V$ curve. Here we will keep two of these parameters constant, and vary $\alpha$. The circuit components used provide a nominal value of $\beta = 1$. Accurate measurements indicate that in fact $\beta = 1.023$. Following Ref. [7] we define $\gamma$ as the inverse of the dimensionless voltage for which the current has fallen to one-half its maximum value. From Fig. 1(c) we find $V_{1/2} = 1.6$ V, so that $\gamma = (I_0\sqrt{L/C})/V_{1/2} = 2.8$, a value close to that used in computer simulations [7]. Here $I_0 = 3$ mA is the maximum of the nonlinear $I$-$V$ curve of Fig. 1(c).

TABLE I. An electrical analog of mechanical systems.

| Mechanical model | Electronic circuit |
|---|---|
| Mass | Capacitance |
| Spring constant $k$ | 1/Inductance |
| Velocity | Voltage |
| Force | Current |
| Friction | Resistance |

The most critical part of the circuit is synthesizing the nonlinear element. The two-JFET (junction field effect transistor) configuration [13] in Fig. 1 has a region of negative differential resistance (NDR) for voltages greater than $\approx$2.5 V. So that the JFETs have NDR behavior for voltages greater than zero volts, we apply a negative voltage $V_{\text{offset}}$ as shown. To model the stick regime, which prevents the "block" from moving backwards, a diode and a voltage source $V_{\text{diode}}$ are placed in parallel with the nonlinear element; a large forward current (force) is then generated if the voltage across the nonlinear element falls below zero.

The velocities of the blocks, which correspond to the voltages at nodes 1 and 2 of Fig. 1, may be directly read by a digital oscilloscope. The blocks' positions may be obtained either by integration of the velocity data, or by measuring the current $I$ through the inductors $L$. By analogy with Hooke's law $f = ky$, the spring stretch $X$ is then determined from $I = L^{-1}X$.

Figure 2 shows time traces of $X_1$, $V_1$ (continuous line), and $X_2$, $V_2$ (dashed line), for several values of $\alpha$, the coupling parameter. The $X$'s correspond to the displacements of the driver springs, $y_1$ and $y_2$, and the voltages $V$ (here offset for clarity) correspond to their respective time derivatives, or velocities $\dot{y}_1$ and $\dot{y}_2$. The square frames on the right side of each time trace present the corresponding dynamics in configuration space, $X_1$ versus $X_2$, and $V_1$ versus $V_2$.

As seen in the left frames of Fig. 2, the circuit evolves between two generic states, *loading* and *unloading*. At the start of the loading stage, the blocks' velocities are zero, i.e., $V_1 = V_2 = 0$. This leads to a voltage difference $V_d$ across the inductor, so that the current into the nonlinear element slowly increases; the circuit is stable but is slowly being driven to the threshold of instability at the crest of the $I$-$V$ curve. When this point is reached, a sudden response (analogous to an avalanche or earthquake) unloads the "stress" built into the system. For a single $L$-$C$ node, this leads to a periodic behavior in time, but even with two nodes, the extra loading stress introduced by neighboring circuits leads to highly complex behavior as a function of the circuit parameters.

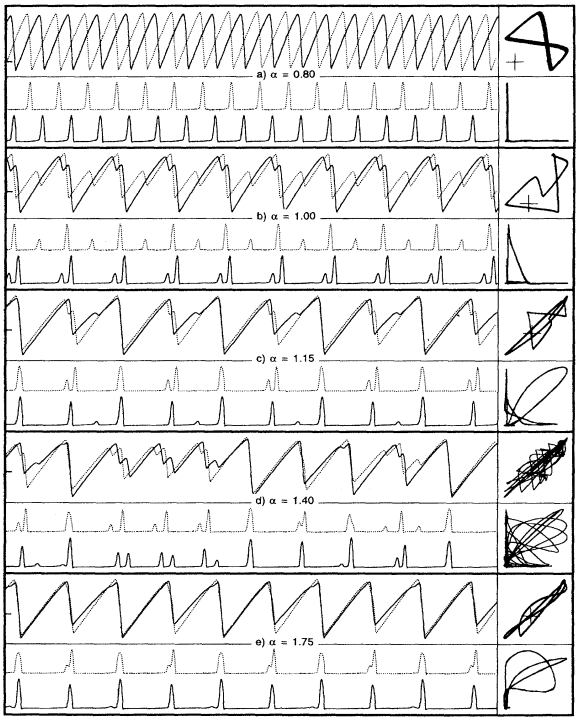


FIG. 2. Time traces of $X_1$, $V_1$ (continuous line), and $X_2$, $V_2$ (dashed line), for several values of $\alpha$, the coupling parameter. The vertical axes have arbitrary units, while the horizontal axis spans 800 $\mu$s. The square frames on the right side of each time trace are the corresponding trajectories in configuration space, $X_1$ vs $X_2$, and $V_1$ vs $V_2$. Zero is marked by a short bar for the $X$ time traces, while a cross indicates the origin of the $X_1$ vs $X_2$ plots.

In the $X_1$ vs $X_2$ plots, accumulation of stress appears as diagonal lines with slopes of about 1. During these loading periods, $X_1$ and $X_2$ increase at the same slow rate, corresponding to the slow stretching of the driving springs while the blocks are stuck. At the top right end of each diagonal line, failure occurs and one (indicated by a roughly vertical or horizontal line) or both (a more complex curve) of the coupled circuits relax. The horizontal and vertical lines, corresponding to one-block slips, are slightly tilted in the $X_1$ vs $X_2$ return maps because of the finite value of the driving voltage.

Variations of the system dynamics, as a function of $\alpha$, can be summarized in a bifurcation diagram. It can be shown [6] that the difference in extension of the two driving springs after a slip event is completely determined by the difference after the previous event. Plotting this difference, $X_2 - X_1$, as $\alpha$ is varied can indicate compactly whether the system is in a periodic, quasiperiodic, or chaotic regime.

Figure 3 shows the bifurcation diagram, obtained by plotting $X_2 - X_1$ at the end of each slip event, versus $\alpha$. The arrows in Fig. 3 correspond to the values of $\alpha$ at which the time traces of Fig. 2 were taken. For

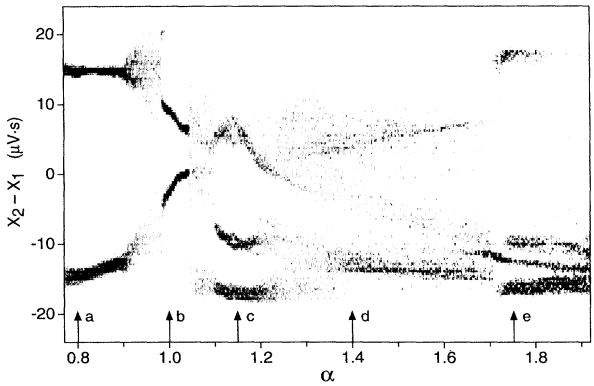


FIG. 3. Experimentally obtained bifurcation diagram. At each of 400 values of $\alpha$, the value of $X_2 - X_1$ at the end of each slip event is plotted, with the grayscale darkness of the image proportional to the probability that after a given slip event, the distance between blocks will be a distance $X_2 - X_1$ apart. There are 107 352 events plotted. Regions with periodic orbits are separated by chaotic regions.

$\alpha = 0.8$ (arrow *a*), the system exhibits a stable period-two orbit. By the *period* of a time trace we mean the number of slip events occurring between identical parts of the time trace. As seen in Fig. 2(a), at the end of each slip (defined by times when *both* velocities have first become zero) the blocks cycle between two possible values of $X_2 - X_1$. In this alternating sequence, one block slips, then the other. This leads to a characteristic "bow tie" shape in the $X_2$ vs $X_1$ plot. The $V_2$ vs $V_1$ plot, however, consists of only two lines, since block one's velocity is zero whenever two's velocity is not, and vice versa. This leads to the two branches of the bifurcation diagram seen for $\alpha < 0.9$. It is interesting to note that this orbit is *not* completely periodic. As seen in Fig. 2(a), the orbit does not repeat itself exactly, and, in Fig. 3, the two branches have significant widths, especially the lower branch. It is not clear whether this represents true chaotic behavior, with a rather tight attractor, or is simply due to experimental noise coupling into a true periodic orbit.

For $\alpha = 1.0$, we again have a period-two orbit, but here, both the time trace itself [Fig. 2(b)] and the bifurcation data (arrow *b*, Fig. 3) appear more periodic. If it is in fact experimental noise which causes the finite widths of traces *a*, this noise must couple into the system differently at different values of $\alpha$. The time traces make it clear that this period-two orbit is different in character than that at $\alpha = 0.8$. A close examination of Fig. 2(b) shows that while one slip is a single-block event, the other involves multiple slips of both blocks at once. The return maps in Fig. 2 are especially useful for determining the periodicity of an orbit. Since each 45° diagonal segment represents the system loading, we can simply count up the number of such segments in the return map to determine the periodicity. We note, for example, that the return maps at both

$a$ and $b$ have two diagonal segments, indicating directly their period-two nature.

Moving on to $\alpha = 1.15$ (arrow $c$, Fig. 3), we come to another periodic regime, this time with a period-three periodic orbit. The time traces of Fig. 2(c) show the very interesting behavior at this value of the coupling. Starting from the left, both blocks slip together as one. The next event consists of both blocks moving, but in alternating fashion. The final event in the cycle is a small slippage of a single block. In Fig. 3, the three branches of the bifurcation diagram again are relatively wide; there is even a hint of the upper two branches themselves bifurcating. The $X_1$ vs $X_2$ plots in Fig. 2(c), however, appear quite narrow. We note, however, that the bifurcation curve consists of data obtained from 16 time traces, separated in time from each other by the 11 s it takes to download them. The data in Fig. 2 are just one 800 $\mu$s time trace. Thus, if there are very slow drifts in the system (on the order of minutes) these drifts would be evident in the bifurcation diagram, but not so in a very short time trace.

At $\alpha = 1.4$ (arrow $d$, Fig. 3), the system has moved into a truly chaotic regime. The bifurcation diagram indicates that essentially any value of $X_2 - X_1$ is attainable by the system, between upper and lower bounds of about $\pm 20$ $\mu$V s.

Finally, at $\alpha = 1.75$ (arrow $e$, Fig. 3), the bifurcation diagram seems to indicate the presence of a period-four orbit, plus some additional interspersed points; however, an examination of the time traces indicates that the system exhibits period-two behavior. In order to resolve this apparent contradiction, we note again that the time traces represent less than a millisecond of data, while the bifurcation diagram presents data on the scale of minutes. Thus, the time traces are a snapshot of the system, while the bifurcation diagram represents the average long-term dynamics. The latter seems to indicate regions of periodicity interspersed among the chaotic orbits. This type of behavior, where periodic orbits are interspersed with occasional brief bursts of chaotic activity, is often referred to as intermittency [12].

It is instructive to compare previous computer simulations with the above experimental results. For $\beta = 1$, no chaotic behavior was found in computer simulations of the two-block system with a velocity-weakening friction law [7] or with a uniform static or dynamic friction law [6]. Thus, the symmetry evidently increases the system stability for a variety of frictional conditions. Our experimental results indicate that this theoretical prediction is *not* robust for physical systems. Even though our circuit has a nominal value of $\beta = 1$, and tested value of $\beta = 1.023$, the circuit exhibits chaotic behavior for much of the range of the coupling parameter $\alpha$. On the other hand, chaotic behavior seems generic for $\beta \neq 1$, and the predictions in this regime appear to describe real systems, even those which are nominally symmetric. The presence or absence of chaos in the slider-block systems is very sensitive to its symmetry. Thus, it appears that any physical system, such as the circuit presented here, is unlikely to have the symmetry required to exhibit nonchaotic behavior. Our experimental bifurcation diagram is qualitatively similar to the computer-generated bifurcation diagrams of Ref. [7], but differs in most quantitative details. A direct comparison is difficult, however, because the theoretical parameters are different from the ones used experimentally. Furthermore, the circuit is driven at a non-negligible voltage, while the model is driven at a vanishingly small velocity.

In summary, our circuit exhibits a very rich dynamics as a function of the coupling strength $\alpha$. The experimentally measured bifurcation diagram indicates that the circuit exhibits alternating regions of periodic and chaotic behavior as $\alpha$ is varied. At large values of $\alpha$, the dynamics appears to exhibit intermittent behavior, with bursts of chaotic behavior. This chaotic behavior was unexpected given the nominal symmetry of our system. Indeed, the bifurcation diagram of our circuit differs in most details from those obtained from computer simulations. These and other issues are currently under study with further experiments as well as computer simulations.


[1] R. Burridge and L. Knopoff, Bull. Seismol. Soc. Am. **57**, 341 (1967).

[2] C. H. Scholz, *The Mechanics of Earthquake Faulting* (Cambridge University Press, Cambridge, 1990).

[3] D. L. Turcotte, *Fractals and Chaos in Geology and Geophysics* (Cambridge University Press, Cambridge, 1992).

[4] P. Bak and C. Tang, J. Geophys. **94**, 15 635 (1989).

[5] J. M. Carlson and J. S. Langer, Phys. Rev. A **40**, 6470 (1989).

[6] J. Nussbaum and A. Ruina, Pure Appl. Geophys. **125**, 629 (1987).

[7] J. Huang and D. L. Turcotte, Nature (London) **348**, 234 (1990); Pure Appl. Geophys. **138**, 569 (1992).

[8] J. Huang and D. L. Turcotte, Geophys. Res. Lett. **17**, 223 (1990); G. Narkounskaia and D. L. Turcotte, Geophys. J. Int. **111**, 250 (1992).

[9] C. H. Scholz, Nature (London) **348**, 197 (1990); **338**, 459 (1990).

[10] J. P. Gollub, E. J. Romer, and J. E. Socolar, J. Stat. Phys. **23**, 321 (1980).

[11] *Proceedings of the First Experimental Chaos Conference,* edited by S. Vohra *et al.* (World Scientific, River Edge, NJ, 1992).

[12] H. L. Swinney, Physica (Amsterdam) **7D**, 3 (1983).

[13] L. O. Chua, J. Yu, and Y. Yu, IEEE Trans. Circ. Syst. **CAS-32**, 46 (1985).

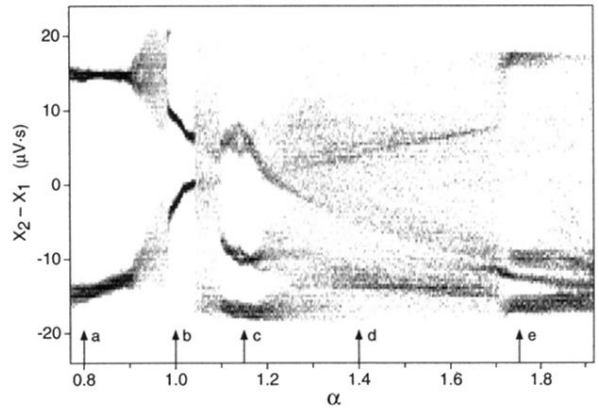


FIG. 3. Experimentally obtained bifurcation diagram. At each of 400 values of $\alpha$, the value of $X_2 - X_1$ at the end of each slip event is plotted, with the grayscale darkness of the image proportional to the probability that after a given slip event, the distance between blocks will be a distance $X_2 - X_1$ apart. There are 107 352 events plotted. Regions with periodic orbits are separated by chaotic regions.